Supplementary Information

Hydrolytic inhibition of α-chymotrypsin by 2,8,14,20-tetrakis(D-leucyl-D-valinamido)resorc[4]arenecarboxylic acid: a spectroscopic NMR and computational combined approach

Gloria Uccello-Barretta,[a*] Federica Balzano,[a] Federica Aiello,[a] Letizia Vanni,[a] Mattia Mori,[b] Sergio Menta,[c] Andrea Calcaterra[c] and Bruno Botta[c]

[a] *Dipartimento di Chimica e Chimica Industriale, Università di Pisa, Via Risorgimento 35, 56126 Pisa, Italy*

[b] *Center for Life Nano Science@Sapienza, Istituto Italiano di Tecnologia, Viale Regina Elena 291, 00161 Roma, Italy*

[c] *Dipartimento di Chimica e Tecnologie del Farmaco, Università degli studi di Roma "La Sapienza", piazzale Aldo Moro 5, 00185, Roma*

Contents

Stereochemical characterization of 1-DD and Suc-AAPF-pNA

***1**-DD in DMSO-d_6*

With regard of the resorcin[4]arene derivative, only one signal for each proton or set of intrinsically equivalent protons was detected in the ^{1}H NMR spectrum (600 MHz, DMSO-d_6, 10 mM, 25°C), with the sole exception of the methoxy groups (Figure 1S), which showed two distinct resonances.

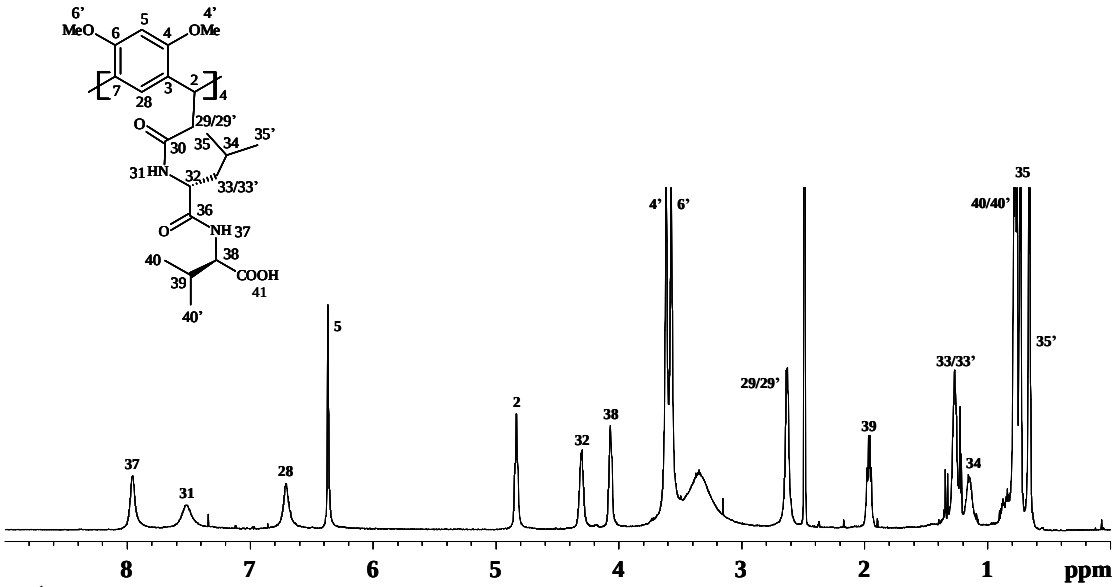

Figure 1S- ^{1}H NMR (600 MHz, DMSO-d_6, 10 mM, 25°C) spectrum of resorcin[4]arene **1**-DD.

All NMR resonances were attributed on the basis of the combined use of several homo- and hetero-correlated scalar and dipolar techniques (COSY, TOCSY, ROESY, HSQC, HMBC) and the corresponding data are collected in Table 1S.

It should be noted that all resonances are characterized by a significant linewidth, which is particularly evident for aromatic protons H-25/H-26/H-27/H-28 and for amidic proton NH-31 of leucine fragment, closer to the aromatic protons. This trend suggests the need to perform experiments at variable temperature, in order to underline decoalescence phenomena. Unfortunately, the solvents employed for the NMR analysis (DMSO-d_6 and D_2O) do not allow performing this kind of analysis.

Preliminarily, the possible occurrence of self-aggregation processes, which could give rise to ambiguous interpretation of ROE data, was probed by comparing the ^{1}H NMR parameters of **1**-DD solutions progressively diluted from 10 mM to 0.1 mM: no changes of the resonances positions or line-widths were detected inside the above said concentration gradient.

Table 1S- ^{1}H NMR signals for **1**-DD (600 MHz, DMSO-d_6, 10 mM, 25°C) (δ, ppm, related to TMS as internal standard; J, Hz).

Proton	δ	m[a]	J
2/8/14/20	4.84	t	2-29= 6.1; 2-29' = 6.1
4'/10'/16'/22'	3.62	s	
5/11/17/23	6.37	s	
6'/12'/18'/24'	3.58	s	
25/26/27/28	6.71	br s	
29/29'	2.63	d	29/29'-2 = 6.1
31	7.51	br s	
32	4.31	m	
33/33'	1.27	m	
34	1.16	m	
35	0.74	d	35-34 = 7.1
35'	0.67	d	35'-34 = 7.1
37	7.96	br s	
38	4.07	t	38-39 = 7.1; 38-37 = 7.1
39	1.96	m	
40	0.79	d	40-39 = 6.4
40'	0.77	d	40'-39 = 6.4
41	12.45	br s	

a- t = triplet; s = singlet; d = doublet; br s = broad singlet; m = multiplet.

The DOSY maps of 0.1 mM and 10 mM solutions of **1**-DD gave the same values of the diffusion coefficients of 1.22×10^{-10} m^2s^{-1}. Therefore, the response both of chemical shifts and diffusion coefficients to concentration gradients allowed us to rule out the occurrence of self-aggregation processes in the macrocycle **1**-DD. On these basis, the dipolar interactions detected in the ROESY maps can be reliably attributed to intramolecular effects.

The conformation of **1**-DD was analyzed starting from the aromatic moieties: the protons H-5 located between the methoxy groups originated dipolar interactions only with the methoxy protons (Figure 2Sa) and the other aromatic protons H-28 showed intense ROEs at the frequency of the methylene protons H-29/29’ (Figure 2Sb) and a very small effect at the methine protons H-2, which demonstrated the strong prevalence of the cone conformation.

The perturbation of the methine proton H-2, lying on the resorcin[4]arene bridge, is responsible for ROEs only at the frequency of the methylene protons H-29/29’ and weak effects on the methoxy groups (Figure 2Sd) are detected, whereas intense ROEs H29/29’-H28 were found (Figure 2Sc), which demonstrated that the methylene protons H29/29’ are directed towards the lower rim of the resorcin[4]arene.

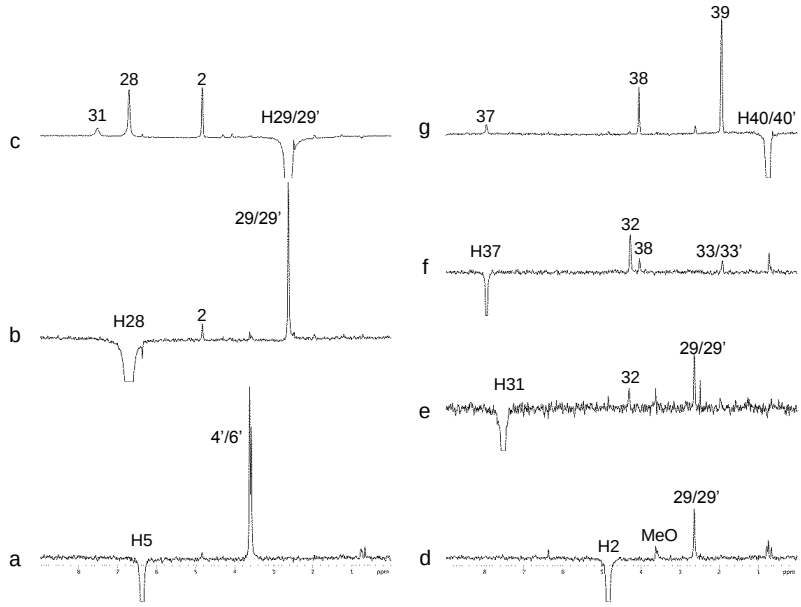

Figure 2S. 2D ROESY traces (600 MHz, DMSO, 25 °C, mixing time 200 ms) corresponding to selected protons of **1**-DD: H-5 (a), H-28 (b), H-29/29' (c), H-2 (d), H-31 (e), H-37 (f), H-40/40' (g).

The amide proton H-31 of the leucine fragment shows dipole-dipole interactions with the methylene protons H-29/29' and a weaker interaction with H-32 (Figure 2Se). Thus, the NH-31 bond is trans with respect to H_{32} and bent at the lower rim of the resorcin[4]arene as the methylene protons H-29/29'. The position of the NH-37 proton of the valine residue was defined on the basis of trace f of Figure 2S, where the ROE H37-H32 was more intense with respect to the ROE H37-H38, to indicate that NH-37 is faced to the bond CH-32 and transoid with respect to the bond CH-38. Finally, the methyl protons of valine produced ROEs only at the frequencies of valine protons (Figure 2Sg).

The two methyl protons of the leucine residue, which are adjacent to the resorcin[4]arene cone structure, are remarkably differentiated in the NMR spectrum (0.74 ppm and 0.67 ppm for H-35 and H-35' respectively) and the origin of such a kind of differentiation can be very well understood by analyzing the ROE effects of Figure 3S: for the methyl group H-35', which is low frequencies shifted, high intensities ROEs with the methine proton H-32 of the leucine residue and the aromatic proton H-5 were detected together with a ROE with only one of the two methoxy groups (named as H-4'). The high frequencies shifted methyl group H-35 (Figure 3S) showed weaker effects on H-32, H-5 and both methoxy groups. Thus, both the two methyl groups of leucine are oriented at the upper rim of the resorcin[4]arene, but H-35 is transoid with respect to the H-32 proton, whereas H-35' is in proximity of the methine proton H-32. It is noteworthy that any ROEs with aromatic protons were not detected in the spectral region including the methyl resonances of the valine residue. Above effects are in keeping with the truncated cone shape of the resorcin[4]arene.

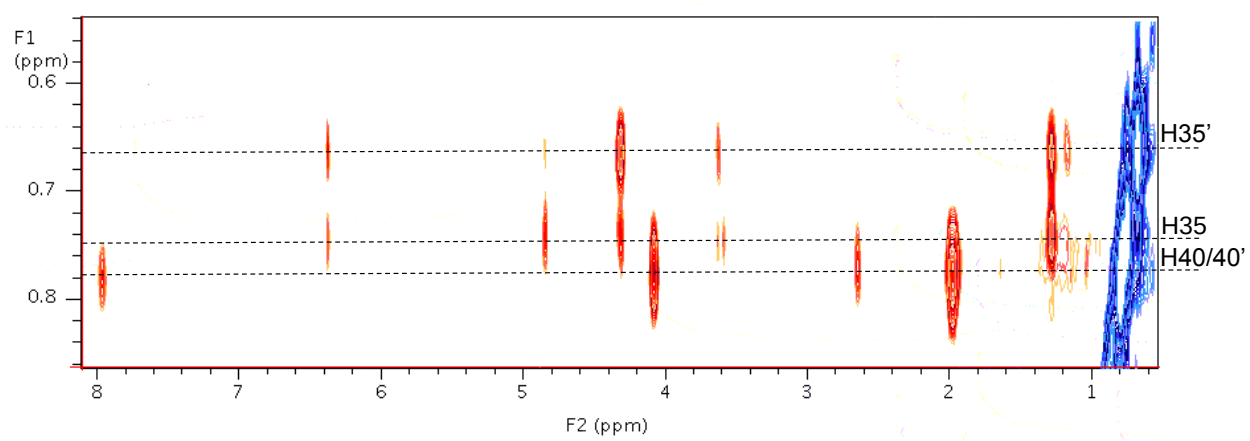

Figure 3S. Expansion of 2D ROESY map (600 MHz, DMSO, 25 °C, mixing time 200 ms) relatively to methyl protons of **1**-DD**.**

***1**-DD in D_2O*

As already discussed in results and discussion, the most significant difference detected in D_2O solution of the resorcin[4]arene regards the structure of the methylene protons H29/29' of the bridge, which are well differentiated as showed in Figure 4S.

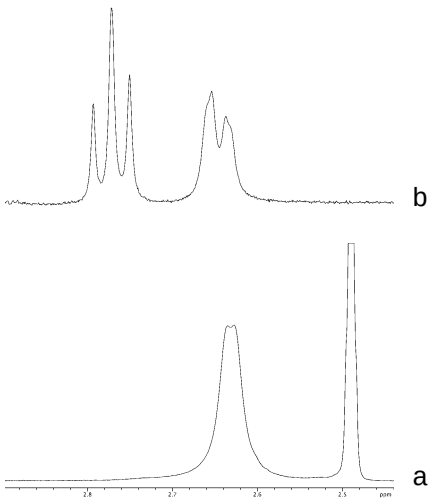

Figure 4S. Comparison of the ^{1}H NMR (600 MHz, 25 °C) spectral regions of the methylene protons H-29/29' of **1**-DD in: a) DMSO-d_6, b) D_2O pH 7.4.

The coupling constant for the H29-C-C-H2 fragment, equal to 11.5 Hz, allowed us to calculate a dihedral angle of 172.1° by using the Karplus relationship[1] (Eq. 1):

$$^3J = A\cos^2\theta - B\cos\theta \qquad (1)$$

where A and B parameters are 10.2 and 1.2, respectively. The $^3J_{H29'\text{-}H2}$ of 3.1 Hz gave the two possible dihedral angles of 52.8° e 119.4°. The ROESY traces of Figure 5S showed that H-29' was nearer to H-2 than H-29 was, allowing us to select the value of 52.8° for the H29'-C-C-H2

fragment. The two protons H-29 and H-29’ were equidistant from the aromatic proton H-28 on lower rim of **1**-DD.

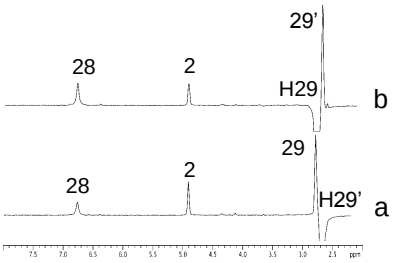

Figure 5S. 2D ROESY traces (600 MHz, D_2O phosphate buffer pH 7.4, 25 °C, mixing time 300 ms) of H-29’ (a) and H-29 (b) protons of **1**-DD.

Suc-AAPF-pNA

The structural characterization was initially conducted also for the *trans* isomer, that is the prevalent species (Fig. 6S); its NMR resonances were attributed on the basis of the combined use of several homo- and hetero-correlated scalar and dipolar techniques (COSY, TOCSY, ROESY, HSQC, HMBC) and the corresponding data are collected in Table 2S.

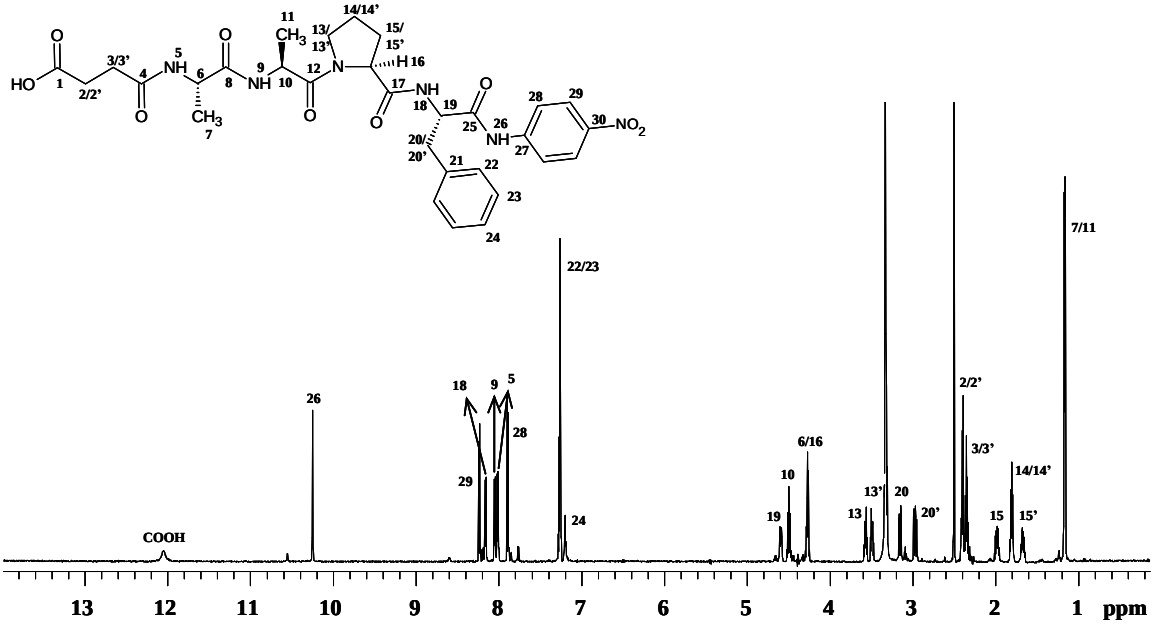

Figure 6S- ^{1}H NMR (600 MHz, DMSO-d_6, 4.5 mM, 25 °C) spectrum of Suc-AAPF-pNA.

Table 2S- ^{1}H NMR signals for *trans*-Suc-AAPF-pNA (600 MHz, DMSO-d_6, 4.5 mM, 25°C) (δ, ppm, related to TMS as internal standard; J, Hz). *Cis* Suc-AAPF-pNA chemical shifts are given in parentheses.

Proton	δ	m[a]	J
COOH	12.04	s	
2/2'	2.38	m	
3/3'	2.34	m	
5	8.01	d	5-6 = 7.5
6	4.26 (4.32)	m	
7	1.16	d	7-6 = 7.1
9	8.04 (7.85)	d	9-10 = 7.0
10	4.48 (4.26)	m	
11	1.15	d	11-10 = 7.1
13	3.55 (3.55)	m	
13'	3.48 (3.48)	m	
14/14'	1.79 (1.66/1.43)	m	
15	1.97 (2.06)	m	
15'	1.66 (1.93)	m	
16	4.26 (4.44)	m	
18	8.15 (8.59)	d	18-19 = 7.5
19	4.60 (4.65)	m	
20	3.14 (3.08)	dd	20-20' = 13.7; 20-19 = 5.1
20'	2.96 (3.08)	dd	20'-20 = 13.7; 20'-19 = 9.6
22	7.25	m	
23	7.25	m	
24	7.19	m	
26	10.24 (10.54)	s	
28	7.89 (7.76)	d	28-29 = 9.0
29	8.22 (8.18)	d	29-28 = 9.0

a- s = singlet; d = doublet; dd = double doublet; m = multiplet.

The conformational analysis started from the amide proton NH-9: the inter-residue ROE Ala-Ala NH9-CH6 was stronger than the intra-residue NH9-CH10 was (Figure 7Sa), which allowed us to establish that the two protons H-9 and H-6 were reciprocally cisoid.

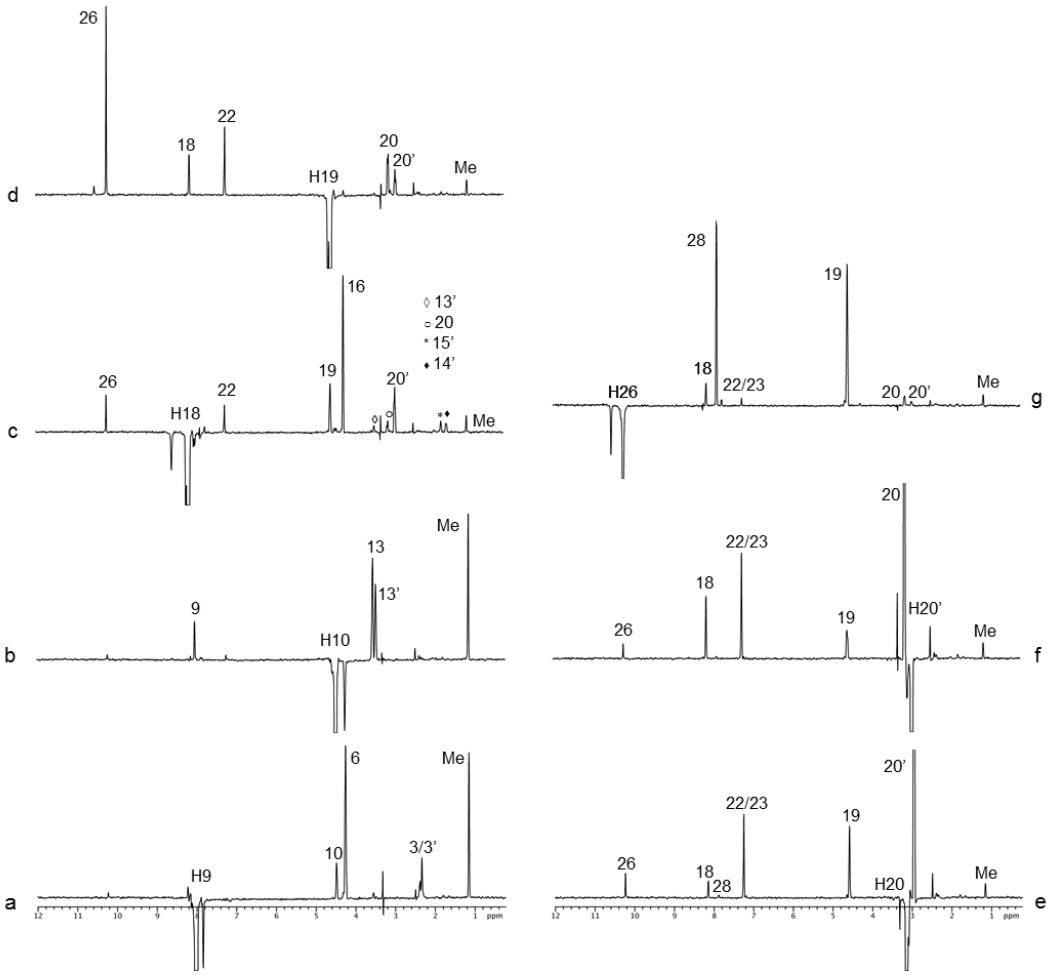

Figure 7S. 2D ROESY traces (600 MHz, DMSO, 25 °C, mixing time 200 ms) corresponding to selected protons of Suc-AAPF-pNA: H-9 (a), H-10 (b), H-18 (c), H-19 (d), H-20 (e), H-20' (f), H-26 (g).

The methine proton H-10 is bent at the two protons H-13 and H-13', nearly equidistant from them (Figure 7Sb). The ROESY trace corresponding to the amide proton NH-18 of the Phe residue showed (Figure 7Sc) strong dipolar interaction with the H-16 proton of Pro and several effects at the frequencies of its benzyl group, whereas a low intensity ROE is detected at the frequency of the adjacent methine proton H-19 and negligible effects are produced on the protons of the p-nitrophenyl group. The proton H-19 is in spatial proximity of the amide proton NH-26 (Figure 7Sd) and of the aromatic protons of the benzyl group. H-19 is cisoid with respect to H-20 ($^3J_{19\text{-}20}$ = 5.1 Hz, $\theta_{19\text{-}20}$ = 41.1°) and transoid with respect to H-20' ($^3J_{19\text{-}20'}$ = 9.6 Hz, $\theta_{19\text{-}20'}$ = 154.5), where H-20' is faced to H-18 (Figure 7Se-f).

The amide proton NH-26 shows (Figure 7Sg) dipolar correlations with selected protons of the aromatic moiety of Phe and the ROE H26-H20 is more intense than the ROE H26-H20' is, where H-20 is cisoid to H-19 and H-20' transoid to it.

After having excluded the possibility of self-aggregation phenomena of Suc-AAPF-pNA, some minor dipolar interactions, such as ROEs between NH-18 and the protons of the pentatomic ring which are on the opposite side with respect to H-16 (Figure 7Sc), were attribute to the presence of

minor populations of the conformer due to the rotation about the C16-C17 bond (Figure 8S). As a matter of fact, both chemical shifts of Suc-AAPF-pNA and its diffusion coefficient, measured by the DOSY technique, were not sensitive to concentration gradients between 4.5 mM till to 0.4 mM. The diffusion coefficient of Suc-AAPF-pNA both in the two solutions was equal to 1.5 x 10^{-10} m^2s^{-1}.

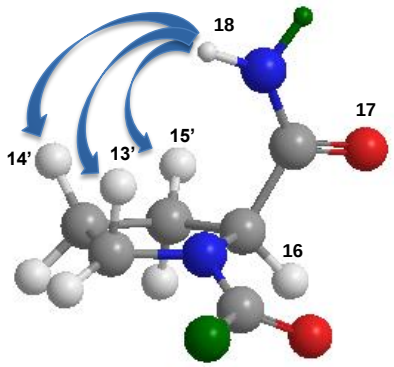

Figure 8S. Three-dimensional representation of the minor conformer of *trans*-Suc-AAPF-pN**A** determined by rotation about the C16-C17 bond. The green balls indicate the not represented portions of the molecule.

A further refinement of the conformational data was achieved by means of cross-relaxation rates (σ_{ij}) determinations for selected proton pairs *ij*. Cross-relaxation rates, which describes the magnetization transfer between the proton pair *ij*,. are functions of the reorientational correlation time (τ_c) of the vector connecting the two spins *i* and *j* and of their distance r_{ij} (Eq. 2):

$$\sigma_{ij} = 0.1\hbar^2\gamma^4 r_{ij}^{-6}\left(\frac{6\tau_c}{1+4\omega^2\tau_c^2} - \tau_c\right) \qquad (2)$$

On the hypothesis of isotropic motion, the ratios between σ values of proton pairs *ij* and *ik* can be correlated to their distances (Eq. 3) and, hence, exploited to exctract average distances between protons.

$$\frac{\sigma_{ij}}{\sigma_{ik}} = \frac{r_{ik}^6}{r_{ij}^6} \qquad (3)$$

The cross-relaxation parameters can be determined in a very simple way on subtracting bi-selective R_{ij}^{bs} and monoselective R_i^{ms} relaxation rates (Eq. 4). Mono- and bi-selective relaxation rates are, respectively, measured by inverting the proton *i* selectively or inverting the proton pair *ij* simultaneously (Figure 9S), leaving unperturbed the other spins, and following the recovery of *i* in time.

$$\sigma_{ij} = R_{ij}^{bs} - R_i^{ms} \quad (4)$$

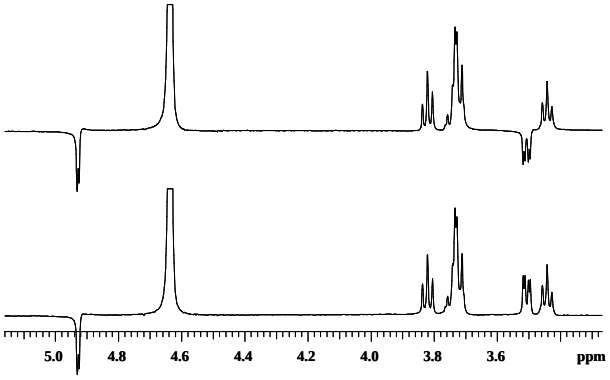

Figure 9S- Mono- and bi-selective inversions.

Our attention was focused on the NH-CH molecular fragment of Phe residue, which are in close proximity of the site involved in the hydrolysis by chymotrypsin. We measured the mono-selective relaxation rates of the two protons NH-18 and CH-19 and the bi-selective relaxation rates which are reported in the Table 3S. As reference distance we assumed $r_{H20\text{-}H20'}$ (1.78 Å), which gave the cross-relaxation parameter of -0.27 s^{-1}.

Table 3S- Mono- and bi-selective relaxation rates (R_i^{ms} and R_{ij}^{bs}, s^{-1}) of H-18 and H-19 protons of trans-Suc-AAPF-pNA. Cross-relaxation parameters (σ_{ij}, s^{-1}) and corresponding distances (r_{ij}, Å).

i	R_i^{ms}	i-j	R_{ij}^{bs}	σ_{ij}	r_{ij}
18	1.56	18-19	1.52	-0.04	2.40
		18-16	1.46	-0.10	2.09
19	1.08	19-18	1.04	-0.04	2.43
		19-20	1.04	-0.04	2.47
		19-20’	1.07	-0.01	2.99
		19-26	0.97	-0.11	2.07
20	2.00	20-20’	1.73	-0.27	1.78

The distances reported in Table 3S, which were calculated by means of Eq. 3 on assuming $\sigma_{H20\text{-}H20'}$ as the reference value, were in optimum agreement with ROE data. The amide proton H-18 is faced to the proton H-16 and transoid to H-19 ($r_{H18\text{-}H19}$ = 2.40 Å, $r_{H18\text{-}H16}$ = 2.09 Å). The short distance between the protons H-19 and H-26 ($r_{19\text{-}26}$= 2.07 Å) well fit their reciprocal intense ROE (Figure 7Sd,g) in comparison with the higher values of $r_{H18\text{-}H19}$ = 2.40 Å. Interestingly, differentiated distances were calculated for the proton pairs H19-H20 and H19-H20’ (2.47 Å and 2.99 Å, respectively), which confirmed that the benzyl proton H-20 was nearer to H-19 than H-20’ was.

As probes of the conformational changes occurring in the stereoisomer *cis* due to the rotation about the Ala-Pro bond, we selected the protons H-18 and H-19, the resonances of which were well differentiated from the corresponding resonances of the prevailing stereoisomer and not superimposed to other signals. We measured the selective relaxation rates which are collected in the Table 4S. Preliminarily, we would observe that the relaxation rates are remarkably higher with respect to *trans*-Suc-AAPF-pNA. As an example, the value of 2.56 s^{-1} was measured for H-18 selectively inverted to be compared with the significantly lower value of 1.56 s^{-1} of the same proton of *trans*-Suc-AAPF-pNA. Analogously, higher was R^{ms} for H-19 (2.22 s^{-1}) in comparison with the value of 1.08 s^{-1} of *trans*-Suc-AAPF-pNA. Such a kind of increases of the relaxation rates may be attributed to the conformational change which occurred in *cis*-Suc-AAPF-pNA with respect to *trans*-Suc-AAPF-pNA and led protons of *cis*-Suc-AAPF-pNA in spatial proximity of a major number of dipolar nuclei, thus giving further contributions to the dipole-dipole relaxation mechanism.

Table 4S- Mono- and bi-selective relaxation rates (R^{ms}_i and R^{bs}_{ij}, s^{-1}) of H-18 and H-19 protons of *cis*-Suc-AAPF-pNA, cross-relaxation parameters (σ_{ij}, s^{-1}) and corresponding distances (r_{ij}, Å).

i	R^{ms}_i	i-j	R^{bs}_{ij}	σ_{ij}	r_{ij}
		18-9	2.33	-0.23	1.94
18	2.56	18-16	2.33	-0.23	1.94
		18-19	2.44	-0.12	2.16
19	2.22	19-26	1.92	-0.30	1.86
28	1.49	28-29	1.43	-0.06	2.43

The distances of Table 4S witnessed such a kind of conformational change. The cross-relaxation parameters for some proton pairs were calculated by means of Eq. 4 from mono- and bi-selective relaxation rates measurements and were referred to the cross-relaxation parameter of the proton pair H28-H29, which were at the known distance of 2.43 Å. A very short distance of 1.94 Å was calculated between the amide proton H-18 of Phe and the amide proton H-9 of Ala, which was the consequence of the rotation about the Ala-Pro linkage and proved that the two side arms were in spatial proximity in the *cis* stereoisomer (Figure 3). The distance H18-H16 is nearly unchanged (1.94 Å in *cis*-Suc-AAPF-pNA and 2.09 Å in *trans*-Suc-AAPF-pNA). A shortening of the distance H19-H26 (1.86 Å in *cis*-Suc-AAPF-pNA and 2.07 Å in *trans*-Suc-AAPF-pNA) and H18-H19 (2.16 Å in *cis*-Suc-AAPF-pNA and 2.40 Å in *trans*-Suc-AAPF-pNA) may result from the steric repulsion between the two syn side chains.

The substrate Suc-AAPF-pNA was characterized also in D_2O (phosphate buffer, pH 7.4): spectral parameters in D_2O are very similar to those in DMSO-d_6 (Figure 10S and Table 5S), which suggested that also the conformational features in the two solvents should be similar.

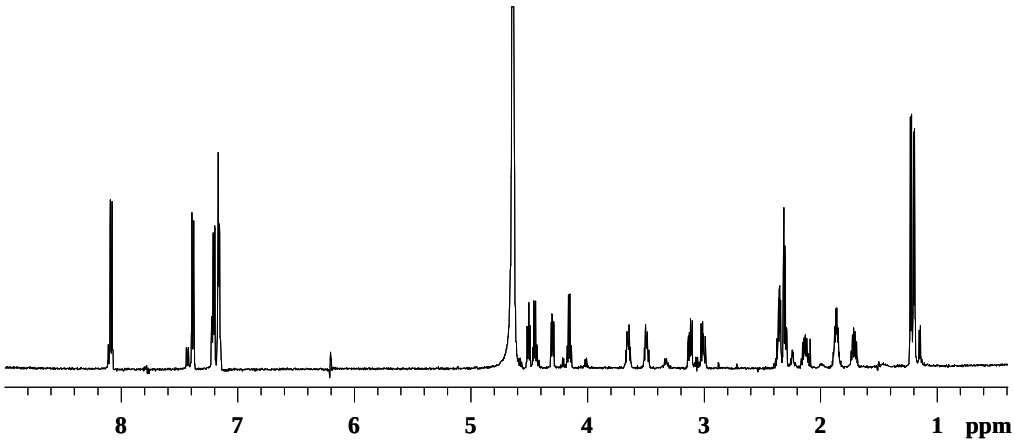

Figure 10S- ^{1}H NMR (600 MHz, D_2O, pH 7.4, 25 °C) spectrum of Suc-AAPF-pNA.

Table 5S- ^{1}H NMR signals for Suc-AAPF-pNA (600 MHz, D_2O pH 7.4, 1.68 mM, 25°C) (δ, ppm, related to TMS as internal standard; J, Hz).

Proton	δ	m	J
2	2.35	m	
3	2.32	m	
6	4.15	q	6-7 = 7.3
7	1.23	d	7-6 = 7.3
10	4.45	q	10-11 = 7.0
11	1.21	d	11-10 = 7.0
13	3.65	dt	13-13' = 10.2; 13-14 = 6.9; 13-14'= 6.9
13'	3.49	dt	13'-13 = 10.2; 13'-14= 6.9; 13'-14'= 6.9
14/14'	1.87	m	
15	2.13	m	
15'	1.72	m	
16	4.30	dd	16-15 = 8.4; 16-15'= 5.7
19	4.51	dd	19-20 = 8.7; 19-20' = 7.1
20	3.12	dd	20-20' = 13.7; 20-19 = 8.7
20'	3.01	dd	20'-20 = 13.7; 20'-19 = 7.1
22	7.20	d	22-23 = 6.9
23	7.17	m	
24	7.17	m	
28	7.39	d	28-29 = 9.2
29	8.09	d	29-28 = 9.2

As we can see by comparing the data reported in Table 2S and in Table 5S, the more relevant differences detected in the two solvents involve the chemical shifts of proline ring and coupling pattern for the fragments H19-C-C-H20 and H19-C-C-H20'.

Table 6S- Diffusion coefficients (D, x 10^{10} m^2/s, DMSO-d_6, 25 °C) calculated for TMS in presence of D_2O.

Sample	D (x 10^{10} m^2/s)
TMS	6.18
TMS + 10 µL D_2O	5.45
TMS + 40 µL D_2O	4.75
TMS + 90 µL D_2O	4.03

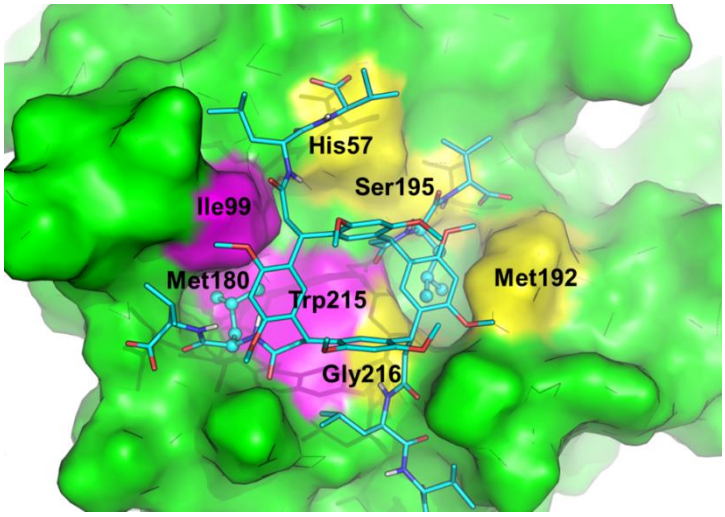

Figure 11S- Hydrophobic clefts (one magenta and one yellow) occupied by two leucine side chains of the dipeptide arms. Hydrophobic residues forming the clefts are labeled. Leucine side chains included within these clefts are showed as sticks and spheres.

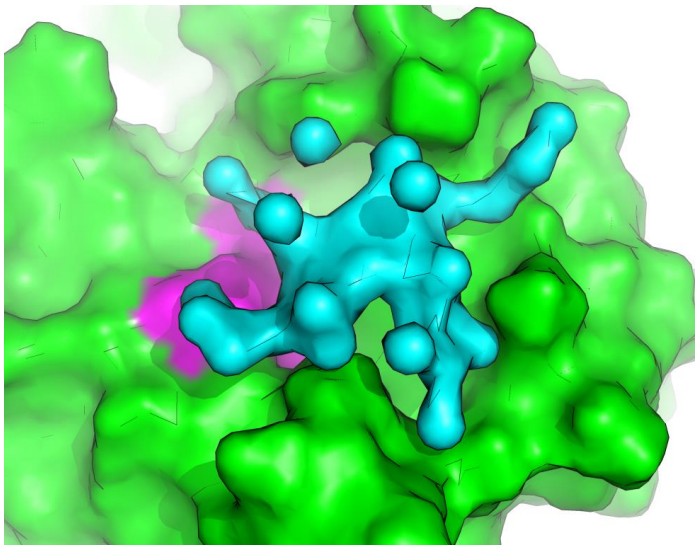

Figure 12S. Shape complementarity between ChT surface and the surface of **1**-DD protons highlighted by the NMR study. ChT is showed as green surface, catalytic residues are colored magenta. **1**-DD is showed as white sticks, while protons H_2, H_5, $H_{29'}$ and H_{32} highlighted by the NMR study are showed as cyan surface.

References

1 (a) Karplus, M. *J. Chem. Phys.* **1959**, *30*, 11-15; (b) Karplus, M. *J. Am. Chem. Soc.* **1963**, 8*5*, 2870-2871; (c) Booth, H. *Progr. Nucl. Mag. Res. Sp.*, Pergamon Press: Oxford **1969**, Vol.5.